H and L Chain Affinity Maturation and/or Fab *N*-Glycosylation Influence Immunoreactivity toward Neutrophil Extracellular Trap Antigens in Rheumatoid Arthritis Synovial B Cell Clones

Elisa Corsiero,* Emanuela Carlotti,* Lucas Jagemann,* Mauro Perretti,[†] Costantino Pitzalis,* and Michele Bombardieri*

We previously showed that anti–neutrophil extracellular trap (NET) rheumatoid arthritis (RA)-rmAbs derived from CD19^{+} B cells within RA human synovial tissues frequently react against NETs. In this study, we aimed to characterize the importance of affinity maturation via somatic hypermutation (SHM) within the Ig variable H (VH) and variable L (VL) chains and Fab–*N*-linked glycosylation in RA synovial B cell clones reactive to NETs and NET-derived Ags such as citrullinated histones. Selected anti-NET RA-rmAbs derived from synovial RA CD19^{+} B cells were subjected to overlap-PCR to generate germline (GL; VH and VL reverted into GL), hybrid clones (VH/VL region reverted into GL), and *N*-glycosylation mutants (N→Q) and analyzed for anti-NETs and citrullinated histones (cit-H2B) immunoreactivity. Anti-NET/cit-H2B immunoreactivity of selected RA-rmAbs was abrogated in the VH and VL GL counterpart. In RA B cell hybrid clone RA015/11.88 and RA056/11.23.2, NET and/or cit-H2B immunoreactivity was solely dependent on SHM in the IgVH region whereas RA B cell hybrid clone RA015/11.91 required affinity maturation of both VH and VL for efficient binding to cit-H2B. In 7/80 RA-rmAb, SHM resulted in ex novo *N*-glycosylation sites in VH and/or VL regions. Removal of Fab-linked glycans in RA056/11.23.2 in the *N*-mutant counterpart resulted in 90% reduction in immunoreactivity to cit-H2B. Thus, SHM in the IgVH and/or VL regions of RA synovial B cells is necessary for the immunoreactivity to NET-Ags. Fab–*N*-linked–glycosylation introduction sites are observed in a minority of anti-NET B cell clones but can strongly influence NET-Ag binding. *The Journal of Immunology*, 2020, 204: 2374–2379.

R heumatoid arthritis (RA) is a joint-destructive inflammatory disorder characterized by breach of self-tolerance and production of anti–cit-peptide/protein Abs (ACPA). In the RA synovium, ectopic germinal centers (GCs) support an autoantigen-driven immune response leading to local ACPA[+]

*Centre for Experimental Medicine and Rheumatology, William Harvey Research Institute, Barts and The London School of Medicine and Dentistry, Queen Mary University of London, London EC1M 6BQ, United Kingdom; and †Centre for Biochemical Pharmacology, William Harvey Research Institute, Barts and The London School of Medicine and Dentistry, Queen Mary University of London, London EC1M 6BQ, United Kingdom

ORCIDs: 0000-0003-2092-6778 (E. Corsiero); 0000-0002-2794-9131 (E. Carlotti); 0000-0002-6412-2619 (L.J.); 0000-0003-2068-3331 (M.P.); 0000-0003-1326-5051 (C.P.).

B cell differentiation (1, 2). Recently, we reported that autoreactive B cells highly mutated within ectopic GCs frequently target cit-histones (cit-H2A/B) contained in neutrophil extracellular traps (NETs) (3). Somatic hypermutation (SHM) within GCs introduces single-point mutations in the variable heavy (VH) and/or variable light (VL) region of unmutated (germline) BCR, thus regulating Ag-driven B cell affinity maturation (4). Additionally, SHM can introduce *N*-glycosylation sites in the VH/VL regions, which can influence Ag binding and/or give an advantage during the selection process to autoreactive B cells (5–7). Circulating and synovial fluid ACPA-IgG are extensively *N*-glycosylated in their Fab domain and this is due to introduction of *N*-glycosylation sites during SHM. The biological effects mediated by the glycans in the variable domain of ACPA-IgG might modulate either the Ag binding and/or BCR signaling or might influence the binding to lectins thus giving survival signals to autoreactive B cells (5, 7, 8). Therefore, additional studies are necessary to enhance our understanding of ACPA-IgG Fab *N*-glycans. In particular, a direct demonstration of the relative contribution of SHM in the VH versus VL region and of the importance of Fab *N*-glycosylation sites for synovial B cell recognition of cit-Ags is missing. Therefore, in this study we characterized the requirement for SHM within the VH and VL regions and of Fab *N*-linked glycosylation for the immunoreactivity to NETs and cit-H2B in RA-rmAbs derived from CD19^{+} B cells obtained from ectopic lymphoid structure (ELS)[+] RA synovial tissues. In particular, we present three different scenarios whereby 1) SHM in the VH region is sufficient for the binding to NETs/cit-H2B; 2) both VH and VL chain affinity maturation contribute to the immunoreactivity; and 3) the introduction of a single

Fab N-glycosylation site account for most of the RA-rmAbs binding to cit-H2B.

Materials and Methods

Generation of RA-rmAbs from ELS+ RA synovial tissue

Eighty RA-rmAbs were generated from single synovial CD19+ B cells, as previously reported (3, 9, 10). Briefly, cDNA from single B cells was amplified by nested PCR using IgV gene-specific primers. Amplified Ig VH and VL genes were then cloned and expressed as rmAbs displaying identical specificity of the original B cells.

Generation of germline, hybrid, and Fab N-linked glycosylation mutant clones by overlap-PCR

To generate germline (GL) and VH/VL hybrid clones, we identified the GL V(D)J gene segment with the highest homology (~90%) from ImMuno-GeneTics, and the mutated VH and/or VL regions were reverted into mature GL counterpart sequence by overlap-PCR as previously described (3, 11). Overlap PCR consisted of two (if J gene GL) or three (if J gene mutated) independent first PCRs followed by a nested overlapping PCR to join the amplicons generated with the first PCRs. As templates for the first reactions, we used plasmids containing the rmAbs clone specific CDR3 regions and plasmids derived from naive B cells, containing the corresponding unmutated VH and VL genes. For hybrid clones, VH or VL regions were reverted into GL. Reverted or single-point mutated IgH and IgL chain PCR products were sequenced to confirm the absence of mutations.

For Fab-linked N-glycosylation mutant (N-mutant), the asparagine residue (N) in the glycosylation site (N-X-S/T) was converted into glutamine residue (Q) by single-point mutation. GL, hybrid, and N-mutant Abs were expressed as previously described (3, 10). For full list of primers used in the overlap-PCRs, see Supplemental Table I.

Immunofluorescence microscopy on NETs

NET preparation and immunofluorescence staining with RA-rmAbs was performed as described (3).

Histone citrullination in vitro

Histone H2B was incubated with rabbit skeletal muscle PAD (7.5 U/mg) in 0.1 M Tris-HCl (pH 7.4), 10 mM CaCl2, and 5 mM DTT for 2 h at 50°C. The reaction was stopped by adding 10 mM EDTA. After incubation, the proteins were stored at −20°C.

ELISA for anti–cit-histones

ELISA plates were coated with cit- or unmodified (native) histones H2B at 10 μg/ml in 1× PBS. RA-rmAbs at 50 μg/ml were transferred into the ELISA plate and incubated for 2 h. Unbound Abs were removed by washing before incubation for 1 h with HRP coupled goat anti-human IgG. Assays were developed using tetramethylbenzidine (TMB) Substrate Reagent Set (BD OptEIA). ODs were measured at 450 nm. ELISA values were expressed as decrease reactivity percentage of the GL clone versus the mature counterpart.

Glycoproteins staining in SDS-polyacrylamide gels

RA-rmAb glycosylation was detected using the Thermo Fisher Scientific Pierce Glycoprotein Staining Kit following the manual's instruction. Ten micrograms of RA-rmAb was loaded on 4–20% SDS-polyacrylamide gel (Bio-Rad). After electrophoresis, the gel was fixed in 50% methanol solution for 30 min. The gel was washed with 3% acetic acid for 10 min and transferred to 25 ml of oxidizing solution for 15 min. After a further wash with 3% acetic acid, the gel was transferred to 25 ml of glycoprotein staining reagent for 15 min. Finally, the gel was transferred to 25 ml of reducing solution for 5 min. After extensive washes with 3% acetic acid and then ultrapure water the glycoproteins appeared as magenta bands.

Ultra-high-pressure liquid chromatography analysis

The ultra-high-pressure liquid chromatography (UHPLC) analysis on RA-rmAbs F(ab′)2 fragment was performed as described in (12) using a Dionex Ultimate 3000 (Thermo Fisher Scientific). Glycan peaks and glycosylation-derived traits were described as reported in (13).

RA synovial tissue transplantation into SCID mice

RA SCID chimeras were established as previously described (1). Sera and synovial grafts were harvested 3 wk posttransplantation and analyzed for IgG ACPA and histology, respectively.

Synovial tissue histological characterization of lymphocytic aggregates

Sequential paraffin-embedded 3-μm sections of synovial tissue were stained for the markers CD3 (1:80 dilution; DAKO), CD20 (1:50 dilution; DAKO), and CD138 (1:50 dilution; DAKO) following routine H&E staining to classify the lymphocytic infiltration as aggregate or diffuse, as previously reported (1).

Detection of human IgG ACPA in mouse sera

ACPA were detected in mouse sera using a commercially available anti–cyclic-cit-Ab (anti-CCP2) ELISA kit (Axis-Shield) following the manufacturer's instructions.

Computational prediction of N-linked glycosylation site

The N-linked glycosylation consensus sequence asparagine (N)-Xaa-serine (S)/threonine (T) (Xaa = any amino acid except proline) was predicted in both H chain (HC) and L chain (LC) using the NetNglyc 1.0 server (http://www.cbs.dtu.dk/services/NetNGlyc/) that predicts the presence of N-glycosylation sites using artificial networks that assess the sequence context of N-X-S/T sequons (13).

Ab structure modeling

The three-dimensional structure prediction of the RA-rmAbs was obtained using the Rosetta molecular modeling software via a user interface called Rosetta Online Server that Includes Everyone (ROSIE; http://rosie.rosettacommons.org) (14). In particular, the ROSIE Ab interface was used. The three-dimensional structure was visualized using the PyMOL software.

Statistical analysis

Differences in quantitative variables were analyzed by one-way ANOVA using GraphPad Prism 5.01 software. A p value < 0.05 was considered statistically significant.

Results

SHM in VH and VL regions is required for the immunoreactivity of synovial B cells toward NETs

We previously reported that anti-NET RA-rmAbs are characterized by a high mutational load within the VH and VL Ig genes (3). Therefore, to address the importance of affinity maturation within synovial ectopic GCs for the RA-rmAb immunoreactivity, we removed by overlap-PCR the acquired mutations from the Ig V region of 10 selected RA-rmAbs displaying strong reactivity toward NETs (Fig. 1A, Supplemental Table II) (3). We confirmed that the reversion to GL of both VH and VL regions completely abrogated the RA-rmAb reactivity toward NETs (Fig. 1B).

To investigate which variable chains (VH/VL) play a dominant role in conferring the reactivity toward NET Ags, we reverted into GL either the IgVH or the IgVL gene (excluding the CDR3) generating hybrid clones (Fig. 1C). As shown in Fig. 1D, when only the IgVH (hybrid VH) or the IgVL (hybrid VL) gene was reverted to GL, all the clones analyzed displayed almost complete abrogation of NET reactivity.

VH more than VL affinity maturation influence the immunoreactivity of synovial B cells toward cit-H2B

We further analyzed three selected B cell clones (RA015/11.88, RA015/11.91 and RA056/11.23.2) for their reactivity toward cit-H2B in ELISA in the GL (VH and VL) and in hybrid (VH or VL) combinations compared with their in vivo mature counterpart. As shown in Fig. 2, all GL clones significantly reduced their reactivity to cit-H2B (range 67–98%) compared with the mature clones.

Interestingly, among the three B cell clones analyzed, RA015/11.88 and RA056/11.23.2 were solely dependent on SHM in the IgVH chain for cit-H2B reactivity with no reduction in binding when the IgVL region was reverted to GL (Fig. 2). Conversely, in
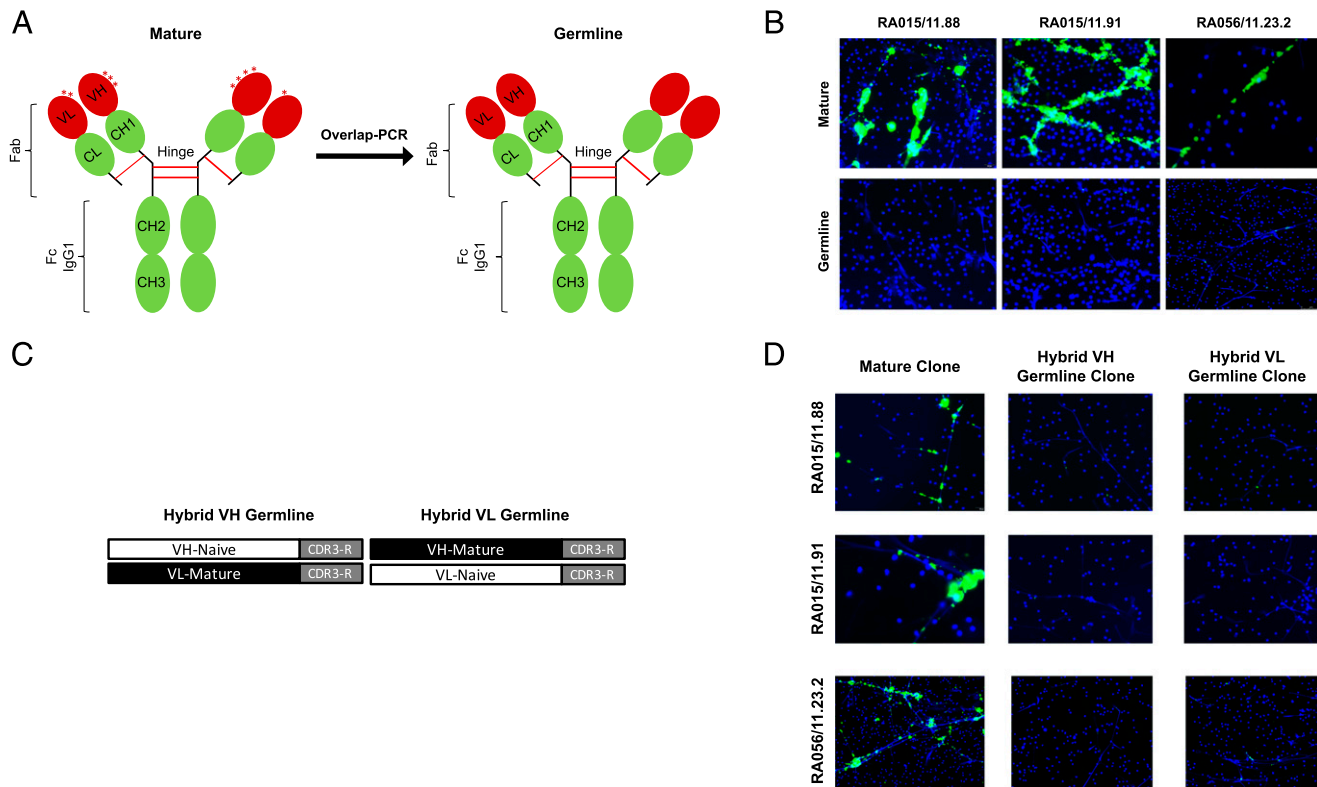
FIGURE 1.   Immunoreactivity toward NETs of germline and hybrid clones. Schematic strategy to generate (**A**) germline VH and VL B cell clones and (**C**) hybrid VH or VL germline B cell clones. Representative pictures of PMA-stimulated neutrophils showing immunoreactivity toward NETs of (**B**) mature versus germline VH and VL RA-rmAbs (green) and (**D**) hybrid VH or VL germline RA-rmAbs (green). NETs were visualized by staining with DAPI (blue). Original magnification ×20.

clone RA015/11.91, both the VH and VL affinity maturation was required for efficient binding to cit-H2B with loss of >60% of the binding to cit-H2B in each of the hybrid clones and 98% reduction in immunoreactivity when both VH and VL were reverted to GL (Fig. 2B).

De novo SHM-dependent Fab N-linked glycosylation in RA synovial B cell clones and its influence to the immunoreactivity of RA-rmAbs to citH2B

We first predicted the presence of the Fab *N*-linked glycosylation and showed that 7 out of 80 RA-rmAbs were characterized by de novo *N*-glycosylation consensus sequences (N-X-S/T) in the V region (Fig. 3A, 3B, Supplemental Table III). A higher prevalence of Fab *N*-glycosylation was observed in anti-NET[+ve] versus anti-NET[−ve] RA-rmAbs (16% versus 4%). Among the seven RA-rmAbs, RA056/11.23.2 displayed Fab *N*-glycosylation sites in both the VH and VL chains. To confirm the presence of *N*-linked glycans in the Fab domain, we screened RA056/11.23.2 RA-rmAb by SDS-PAGE under reducing conditions and observed an increased m.w. in both chains (Fig. 3C) (5). This shift was the result of *N*-linked glycans in the variable regions as confirmed by the presence of glycoproteins in both the VH and VL of RA056/11.23.2 in polyacrylamide gel (Fig. 3C). As expected, Fab *N*-linked glycans were lost in the GL counterpart (Fig. 3C, 3D), confirming that *N*-linked glycosylation consensus sequence is the result of SHM. Next, to investigate whether Fab *N*-glycosylation sites in RA056/11.23.2 influenced its immunoreactivity to cit-H2B, we generated a Fab *N*-linked glycosylation mutant (*N*-mutant) whereby the asparagine residue (N) in the glycosylation site (N-X-S/T) was converted into a glutamine residue (Q). As shown in Fig. 3E, the *N*-mutant RA056/11.23.2 displayed a decreased m.w. due to the loss of *N*-linked glycans. Strikingly, although RA056/11.23.

2 displays a highly mutated VH region, the single *N*-to-Q substitution in *N*-mutant clone almost completely abrogated (90% reduction) the immunoreactivity to cit-H2B (Fig. 3F), suggesting that in this clone Fab *N*-linked glycosylation solely influenced the binding to cit-Ags.

To confirm the presence in vivo of Fab *N*-linked glycosylation in IgG-ACPA autoantibodies from RA synovial B cells, we analyzed the Fab *N*-linked glycans content of human ACPA IgG from in vivo chimeric human RA/SCID mouse model. In this model, SCID mice were transplanted with ELS[+] synovial grafts from ACPA[+] RA patients leading to the detection of high levels of circulating human ACPA IgG (Fig. 3G, 3H) (1). In keeping with data on RA-rmAbs from single synovial B cell clones, the Fab domain of IgG-ACPA from the Hu-RA/SCID mice was significantly *N*-linked glycosylated, confirming that glycosylation sites are acquired during the synovial GC response (Fig. 3I).

Discussion

ELS in the synovium of RA patients are functional sites supporting B cell affinity maturation into high-affinity autoantibody-producing cells. Previously, we demonstrated that highly mutated RA synovial B cells exhibited reactivity toward Ags released by NETs, mainly cit-histones H2A/H2B (3). Importantly, we provided preliminary evidence that the anti-NET immunoreactivity was completely dependent on SHM in the variable regions (3). In this work, we dissected the respective importance of SHM in the HC and LC and the insertion of Fab *N*-linked glycosylation sites (5, 6) for the immunoreactivity against NETs and NET-derived autoantigens. First, we confirmed that the anti-NET immunoreactivity was completely lost in the GL counterpart whereas the anti–cit-H2B immunoreactivity was reduced by over 60%. Recent studies have shown that SHM in the HC/LC interface, distant from the region
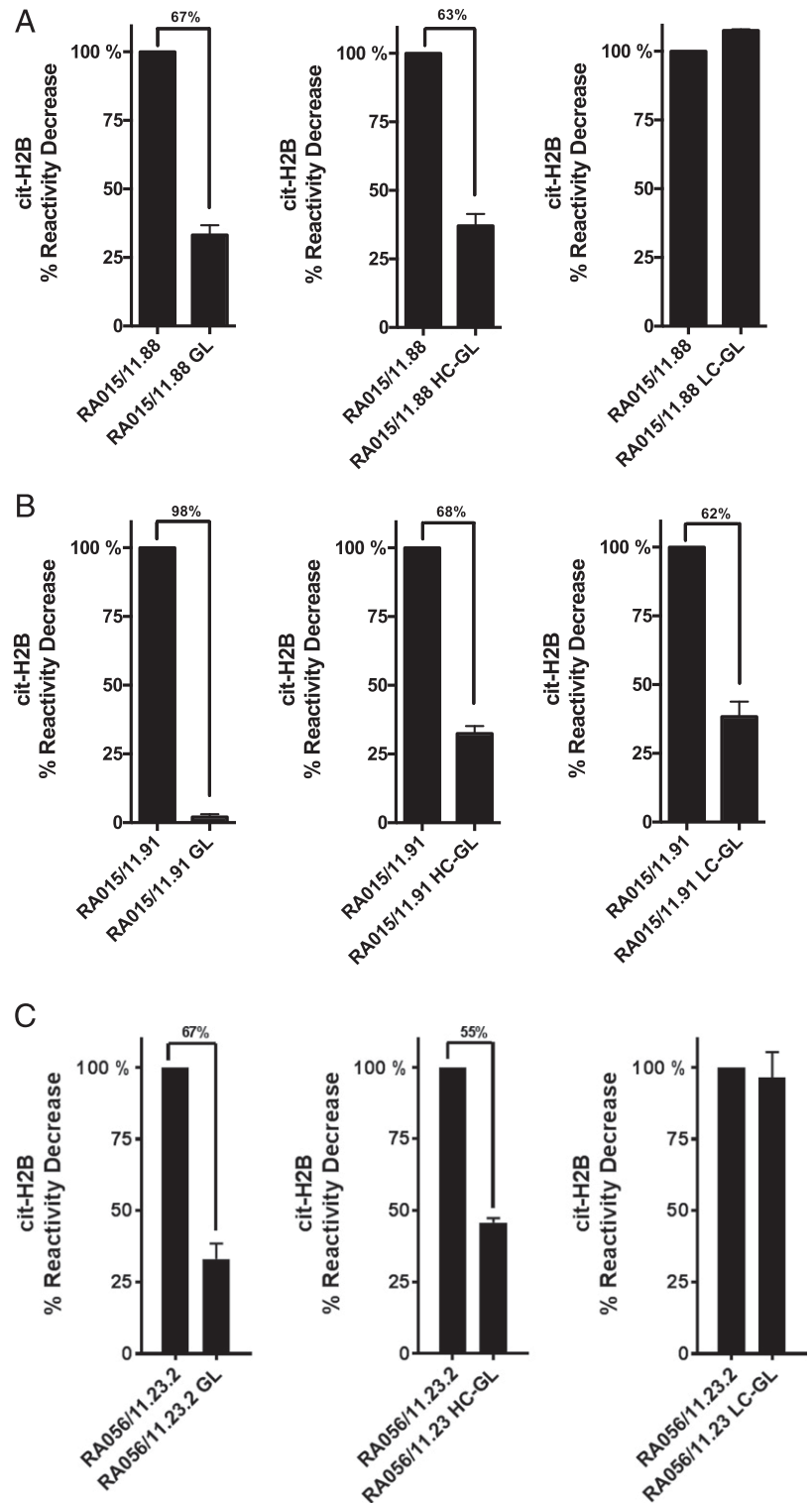
FIGURE 2. Immunoreactivity toward cit-histone H2B of germline and hybrid clones. Binding of the RA-rmAbs GL and hybrids to in vitro cit-histone H2B tested by ELISA for RA-rmAbs RA015/11.88 (**A**), RA015/11.91 (**B**), and RA056/11.23.2 (**C**). Results are expressed as percentage in reactivity decrease compared with the mature clone. Numbers on top of the graph indicate the percentage of decrease reactivity.

of contact between Ag/Ab, play an important role in the high-affinity recognition of the Ag (15). Moreover, it was recently proposed that SHM could generate new reactivity and/or poly-reactivity toward cit-Ags, causing epitope spreading in the ACPA response (16–18). Thus, SHM seems to have a central role not only in the ACPA but overall in autoantigen response. In this study, to dissect the importance of SHM in the individual HC and LC to specifically NET Ag binding, we reverted into GL either the HC or LC of selected anti-NET B cell clones. In particular, we described three different mAbs as representative of three scenarios:

1) SHM in the VH region is sufficient for Ag binding; 2) SHM in both VH and VL chain contribute to the NET/cit-H2B immuno-reactivity; and 3) Fab N-glycosylation influences the RA-rmAb binding to citH2B. We showed that SHM in the HC of two clones (RA015/11.88 and RA056/11.23.2) had a predominant role in NET/cit-H2B binding, whereas SHM in the LC was critical for the binding of clone RA015/11.91. These data strongly suggest that the anti-NET/cit-histones reactivity is dependent on SHM on either/both the HC and LC and is probably acquired during B cells affinity maturation within synovial ectopic GCs. It may still be
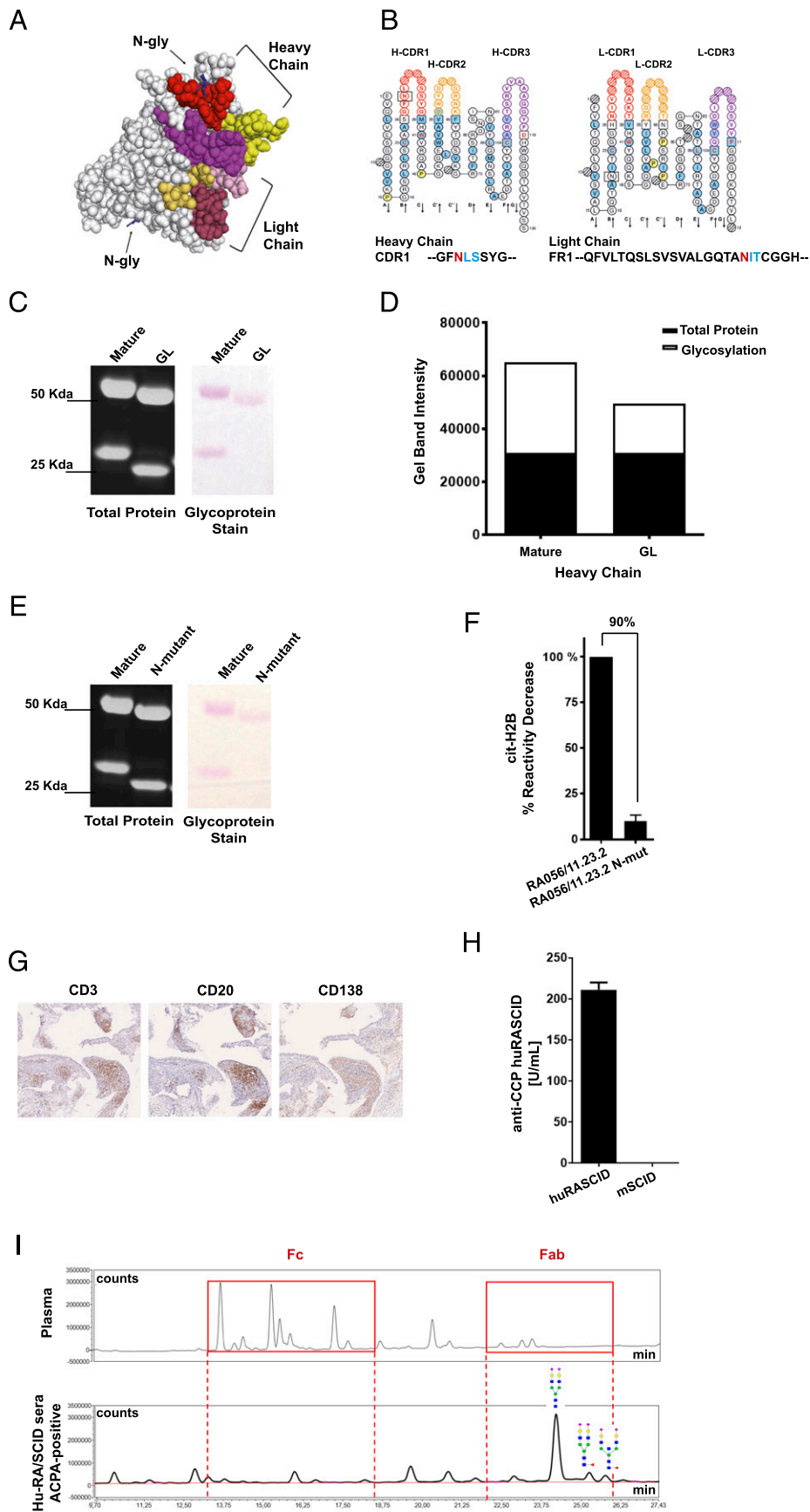
FIGURE 3. Importance of SHM for Fab *N*-linked glycosylation in RA056/11.23.2. (**A**) three-dimensional structure prediction of the RA056/11.23.2 rmAb showing the *N*-glycosylation sites in the V region. CDR regions are shown in color. (**B**) ImMunoGeneTics Collier de Perles (19) of the RA056/11.23.2 rmAb showing the position of the *N*-glycosylation consensus sequence in the HC-CDR1 and LC-framework region 1 (LC-FR1). (**C**) SDS-polyacrylamide gel showing both total protein and glycoprotein staining of the RA056/11.23.2 rmAb. The residual glycoproteins observed in the HC is due to the Fc-glycosylation of the RA-rmAb. HC molecular mass = 50 kDa; LC molecular mass = 25 kDa. Glycans appear as magenta bands. (**D**) Densitometry analysis of the glycoprotein staining. (**E**) SDS-polyacrylamide gel showing both total protein and glycoprotein staining of the *N*-mutant RA056/11.23.2. (**F**) Binding of the *N*-mutant RA056/11.23.2 to cit-H2B tested by ELISA. Results are expressed as percentage in reactivity decrease compared with the mature clone. Number on top of the graph indicates the percentage of decrease reactivity. (**G**) Representative pictures of ELS+ RA synovial tissue (transplanted into SCID mice) paraffin-embedded sections stained for CD3 (T cells), CD20 (B cells) and CD138 (plasma cells). Original magnification ×10. (**H**) Levels of circulating human ACPA-IgG measured by ELISA in the human RA/SCID mice. (**I**) UHPLC chromatograms of the *N*-glycans from human plasma (used as control; top spectra) and from ACPA+ SCID sera (bottom spectra) showing *N*-glycosylation in the Fab domain of ACPA-IgG isolated from SCID sera. Red boxes highlight the *N*-glycans in the Fc (left box) and Fab (right box).

possible that other homologous GL V(D)J from other natural occurring Abs exist; however, we believe the possibility of such a scenario as extremely low. Additionally, because one of the anti-

NET RA-rmAbs is an IgM (RA015/11.88), we have not formally excluded that this clone might retain binding when expressed in a pentameric form.

Recent studies showed that ACPA-IgG in the serum of RA patients are characterized by an increased Fab N-linked glycosylation introduced by affinity maturation that could modulate the Ag binding or give a selective advantage to autoreactive B cells (5–7). Therefore, we analyzed the anti-NET$^+$ rmAbs and reported that a higher prevalence of Fab N-linked glycosylation sites was observed in anti-NET$^+$ versus anti-NET$^-$ rmAbs in the autoreactive B cell compartment. In particular, clone RA056/11.23.2 showed the presence of Fab N-linked glycans in the HC-CDR1 and LC–framework region 1, which were lost in the GL counterpart, confirming that the N-linked glycosylation sites are acquired during B cell affinity maturation. This phenomenon may represent either the acquisition of N-glycosylation sites in synovial GCs or the preferential accumulation of N-glycosylated memory B cells from the peripheral compartment in the presence of ELS. Additionally, in our study, Fab N-linked glycosylation in the CDRs but not FRs was critical for Ag binding, as demonstrated in HC–GL hybrid clone RA056/11.23.2 in which the loss of the N-glycosylation site after reversion into GL within the H-CDR1 but not of L-FR1 affected the Ag binding. These data demonstrate that Fab N-linked glycosylation can play a direct role in the binding to cit-H2B and could be a useful tool for modulating Ab/Ag binding affinity. Further work should be performed on the comparison of N-linked glycosylation acquired at the local site of inflammation in the synovium versus those described in IgG-ACPA obtained from peripheral blood or synovial fluid of RA patients.

We also confirmed that Fab N-linked glycosylation was taking place in vivo in the RA synovium by engrafting GC$^+$ RA synovium into SCID mice, where we showed the presence of Fab N-linked glycans in the circulating ACPA isolated from the SCID sera. It remains to be established whether the type of N-linked glycans acquired at the local site of inflammation is different from the ones developed in the periphery. Thus, we cannot exclude that the glycosylation in the V region of circulating anti-NET Abs could contribute mainly to B cell survival more than influencing the Ag binding, as recently shown from Lloyd and colleagues (7).

Overall, our results highlight the importance of clonal B cell selection and affinity maturation through SHM within RA synovial GCs for the development of NET-binding autoantibodies and provide insights into the mechanisms driving local autoimmunity within the RA joints.

Acknowledgments

Disclosures

The authors have no financial conflicts of interest.

References

1. Humby, F., M. Bombardieri, A. Manzo, S. Kelly, M. C. Blades, B. Kirkham, J. Spencer, and C. Pitzalis. 2009. Ectopic lymphoid structures support ongoing production of class-switched autoantibodies in rheumatoid synovium. *PLoS Med.* 6: e1.
2. Scheel, T., A. Gursche, J. Zacher, T. Häupl, and C. Berek. 2011. V-region gene analysis of locally defined synovial B and plasma cells reveals selected B cell expansion and accumulation of plasma cell clones in rheumatoid arthritis. *Arthritis Rheum.* 63: 63–72.
3. Corsiero, E., M. Bombardieri, E. Carlotti, F. Pratesi, W. Robinson, P. Migliorini, and C. Pitzalis. 2016. Single cell cloning and recombinant monoclonal antibodies generation from RA synovial B cells reveal frequent targeting of citrullinated histones of NETs. *Ann. Rheum. Dis.* 75: 1866–1875.
4. Victora, G. D., and M. C. Nussenzweig. 2012. Germinal centers. *Annu. Rev. Immunol.* 30: 429–457.
5. Rombouts, Y., A. Willemze, J. J. van Beers, J. Shi, P. F. Kerkman, L. van Toorn, G. M. Janssen, A. Zaldumbide, R. C. Hoeben, G. J. Pruijn, et al. 2016. Extensive glycosylation of ACPA-IgG variable domains modulates binding to citrullinated antigens in rheumatoid arthritis. *Ann. Rheum. Dis.* 75: 578–585.
6. van de Bovenkamp, F. S., N. I. L. Derksen, P. Ooijevaar-de Heer, K. A. van Schie, S. Kruithof, M. A. Berkowska, C. E. van der Schoot, H. IJspeert, M. van der Burg, A. Gils, et al. 2018. Adaptive antibody diversification through N-linked glycosylation of the immunoglobulin variable region. *Proc. Natl. Acad. Sci. USA* 115: 1901–1906.
7. Lloyd, K. A., J. Steen, K. Amara, P. J. Titcombe, L. Israelsson, S. L. Lundström, D. Zhou, R. A. Zubarev, E. Reed, L. Piccoli, et al. 2018. Variable domain N-linked glycosylation and negative surface charge are key features of monoclonal ACPA: implications for B-cell selection. *Eur. J. Immunol.* 48: 1030–1045.
8. Vergroesen, R. D., L. M. Slot, B. D. C. van Schaik, M. T. Koning, T. Rispens, A. H. C. van Kampen, R. E. M. Toes, and H. U. Scherer. 2019. N-glycosylation site analysis of citrullinated antigen-specific B-cell receptors indicates alternative selection pathways during autoreactive B-cell development. *Front. Immunol.* 10: 2092.
9. Corsiero, E., L. Jagemann, M. Perretti, C. Pitzalis, and M. Bombardieri. 2018. Characterization of a synovial B cell-derived recombinant monoclonal antibody targeting stromal calreticulin in the rheumatoid joints. *J. Immunol.* 201: 1373–1381.
10. Corsiero, E., L. Jagemann, M. Bombardieri, and C. Pitzalis. 2018. Generation of recombinant monoclonal antibodies from single B cells isolated from synovial tissue of rheumatoid arthritis patients. *Methods Mol. Biol.* 1845: 159–187.
11. Tiller, T., E. Meffre, S. Yurasov, M. Tsuiji, M. C. Nussenzweig, and H. Wardemann. 2008. Efficient generation of monoclonal antibodies from single human B cells by single cell RT-PCR and expression vector cloning. *J. Immunol. Methods* 329: 112–124.
12. Hafkenscheid, L., A. Bondt, H. U. Scherer, T. W. Huizinga, M. Wuhrer, R. E. Toes, and Y. Rombouts. 2017. Structural analysis of variable domain glycosylation of anti-citrullinated protein antibodies in rheumatoid arthritis reveals the presence of highly sialylated glycans. *Mol. Cell. Proteomics* 16: 278–287.
13. Gupta, R., E. Jung, and S. Brunak. 2004. Prediction of N-glycosylation sites in human proteins. NetNGlyc 1.0 Server, Department of Bio and Health Informatics, Technical University of Denmark, Kongens Lyngby, Denmark. Available at: http://www.cbs.dtu.dk/services/NetNGlyc/. Accessed: November 2, 2015.
14. Lyskov, S., F. C. Chou, S. Ó. Conchúir, B. S. Der, K. Drew, D. Kuroda, J. Xu, B. D. Weitzner, P. D. Renfrew, P. Sripakdeevong, et al. 2013. Serverification of molecular modeling applications: the Rosetta online server that includes everyone (ROSIE). *PLoS One* 8: e63906.
15. Cisneros, A., III, R. S. Nargi, E. H. Parrish, C. M. Haliburton, J. Meiler, and J. E. Crowe, Jr. 2019. Role of antibody heavy and light chain interface residues in affinity maturation of binding to HIV envelope glycoprotein. *Mol. Syst. Des. Eng.* 4: 737–746.
16. Kongpachith, S., N. Lingampalli, C. H. Ju, L. K. Blum, D. R. Lu, S. E. Elliott, R. Mao, and W. H. Robinson. 2019. Affinity maturation of the anti-citrullinated protein antibody paratope drives epitope spreading and polyreactivity in rheumatoid arthritis. *Arthritis Rheumatol.* 71: 507–517.
17. Elliott, S. E., S. Kongpachith, N. Lingampalli, J. Z. Adamska, B. J. Cannon, R. Mao, L. K. Blum, and W. H. Robinson. 2018. Affinity maturation drives epitope spreading and generation of proinflammatory anti-citrullinated protein antibodies in rheumatoid arthritis. *Arthritis Rheumatol.* 70: 1946–1958.
18. Titcombe, P. J., G. Wigerblad, N. Sippl, N. Zhang, A. K. Shmagel, P. Sahlström, Y. Zhang, L. O. Barsness, Y. Ghodke-Puranik, A. Baharpoor, et al. 2018. Pathogenic citrulline-multispecific B cell receptor clades in rheumatoid arthritis. *Arthritis Rheumatol.* 70: 1933–1945.
19. Ruiz, M., and M. P. Lefranc. 2002. IMGT gene identification and Colliers de Perles of human immunoglobulins with known 3D structures. *Immunogenetics* 53: 857–883.